Transilvania University of Brasov
FACULTY OF MECHANICAL ENGINEERING

COMAT 2020 & eMECH 2020

Brasov, ROMANIA, 29-31 October 2020

INVESTIGATION OF FATIGUE CRACKS IN ALUMINUM ALLOYS USING ULTRASOUND AND ELECTROMAGNETIC METHODS

Rozina Steigmann[1], Nicoleta Iftimie[1], Gabriel Silviu Dobrescu[1], Mariana Domnica Stanciu[2], Mihail Liviu Craus[1,3], Catalin Ciobanu[1,4]

[1] National Institute of R&D for Technical Physics, Nondestructive Testing Department, Iasi, Romania
[2] Transilvania University, Faculty of Mechanical Engineering, Brasov, Romania
[3] Joint Institute for Nuclear Research, Dubna, Russia
[4]Gheorghe Asachi Technical University, Faculty of Mechanical Engineering, Iasi, Romania
E-mail: steigmann@phys-iasi.ro, niftimie@phys-iasi.ro

Abstract: *The paper presents the methods for nondestructive evaluation of aluminum alloy in order to be used as support for thermal barrier coating. Ultrasound methods are used to determine the mechanical properties. Resonant Ultrasound Spectroscopy is simulated in order to determine the influence of possible inhomogeneities in support plate over the resonance frequencies. The eigenfrequencies are influenced by the microstructure of the material. Also, a new architecture of an electromagnetic sensor in 2D structure is designed and developed in order to estimate the location of a discontinuity below the surface of a conductive material. The study of the dependence of the field distribution on the number and position of the reception coils against the discontinuity was carried out using FDTD. Spatial resolution has been improved using a known super resolution algorithm. The 2D structure was tested for the detection of subsurface discontinuities induced in Al2024 samples subjected to cyclic loading.*
Keywords: *aluminum alloy, thermal barrier coating, nondestructive evaluation, eddy current, ultrasound*

1. INTRODUCTION

Thermal barrier coatings (TBC) are used for the improvement of materials submitted to high temperature. TBC over aluminum alloys used in gas turbines or engine components not only offers thermal protection but also can reduce engine emission [1]. The return of aluminum in the “lights of stage” is due to its possible coatings with rare earths elements that improve the physical and chemical properties.
The phase composition and phase transformations during solidification and thermal treatments are still hard to follows for aluminum alloys [2]. Numerous phase diagrams were developed till now [3], but for multicomponent alloys system they are difficult to be found. Because aluminum alloys are the most used material for structures in automotive industry, their *behavior before and after production* must be determined [4]. Critical IC engine components such as piston heads, fire decks, and exhaust manifolds need quality control and careful maintenance [5] in order to avoid fatigue cracks leading to structural failure. Al–Si–Mg type 2024 alloy is widely used in automotive critical applications due to their moderate strength, lightweight, wear resistance, and good corrosion resistance [6]. During functioning of the engine, before thermal effects, surface damage and cracking at the contact interface can occurs due to vibration [7].
Multiple testing methods have proven their effectiveness in the detection of different defects and damages in Al alloy structures. The most used are based on ultrasonic C-scan inspections but without the sizing ability for different crack depth to sample thickness ratios [8], thermoelastic stress analysis (TSA), acoustic emission (AE) with aim to detect the growth of small cracks [9], digital image correlation (DIC), electronic speckle pattern interferometry (ESPI), electrical resistance and strain gauges described in [10], as different destructive methods to measure damage defined as the effective surface density of micro-cracks. For ideal cracks placed on surface or subsurface, using eddy current method, requires only knowledge of the crack's depth.
The dimensions of the aluminum alloy parts (piston heads, fire decks, and exhaust manifolds), as well as the places where these are used in automotive industry, made that the testing methods shall use miniaturized sensors or arrays of sensors in order to improve the resolution of testing and to reduce the signal post processing time.
The paper presents a 2D architecture in configuration of 5x5 identical reception sensors in order to detect and characterize fatigue cracks into a slab of aluminum 2024 alloy, as precursor for TBC coating, usually used in automotive components. The simulation of eigenfrequencies foreseen the resonant frequencies for the further Resonant Ultrasound measurements. The electromagnetic sensor allows the rapid measurements of the studied samples and signal post processing is carried out using a superresolution algorithm in order to increase the spatial resolution.

2. STUDIED SAMPLES

Samples were machined from a thick sheet of Al 2024 alloy (Figure 1).

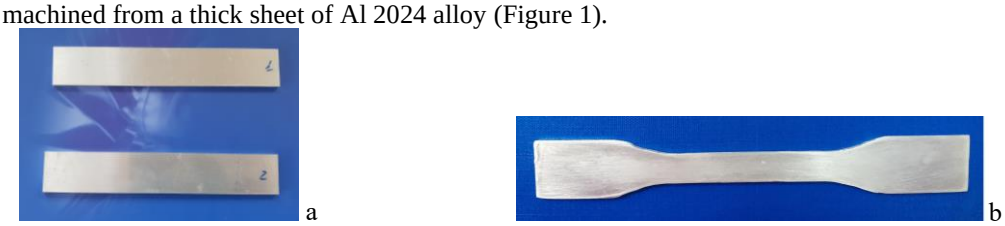

a b

Figure 1: Studied samples: a) for ultrasound measuring; b) for fatigue testing.

The elastic properties of the sample's were determined by ultrasound pitch-catch procedure [11], measuring longitudinal C_L and transversal C_T velocities in different points on the both faces of the samples (Table 1).

Table 1: Studied samples characteristics determined by ultrasound measurements [11]

Sample	ρ [g/cm^3]	C_L [m/s]	C_T [m/s]	ν	E [GPa]	G [GPa]
Al 1	2.772	7657	2775	0.33	74.21	21.24
Al 2	2.778	7516	2867	0.33	71.34	22.8

The emission ultrasound sensor is applied on a face of the sample over a Perspex® delay line with 20 mm height. The emission impulses are delivered by a PR 5077 Square Wave Pulser Receiver Panametrics which also receive the measured signal, amplifies and forward it to digital oscilloscope for reading and acquiring.
Fatigue tests have been performed according to standard ASTM B646 – Fracture toughness testing of aluminum alloys [12] by using the system for the analysis of the fatigue behavior of the structures, Series 1451, K22305 at Transylvania University of Brasov, under cyclic loading using a test frequency of 2 Hz at room temperature. The amplitude of loading was 150MPa determined by strain gauge according to [12], until the fatigue cracks appears opened at the surface detected by a camera that records the crack evolution over time. Once the crack has appeared, the residual fatigue life can be determined according to Paris's law [13]

$$da / DN = C(\Delta K)^m \quad (1)$$

where N are the cycles number, C=1.1x1010 and m=2.589 are materials constants obtained at fatigue testing, ΔK is the amplitude of stress intensity factor, thus $N = \int_{a_0}^{a_c} \frac{1}{C(\Delta K)^m} da$, a0 is the initial length of the crack and ac is the critical length.
The Resonant Ultrasound Spectroscopy [14] has been simulated in order to emphasize the behavior of studied sample under mechanical loading in the presence of an inherent fatigue crack. Figure 2 presents shows the vibration modes for sample obtained by simulation, for the frequencies between 120kHz and 200kHz for an aluminum plate containing an inhomogeneity considered as an inherent fatigue crack (a), the results of simulation of deformations for an extensional modes (b), and a flexural modes (c), obtained using the finite element method using SolidWorks 2018.

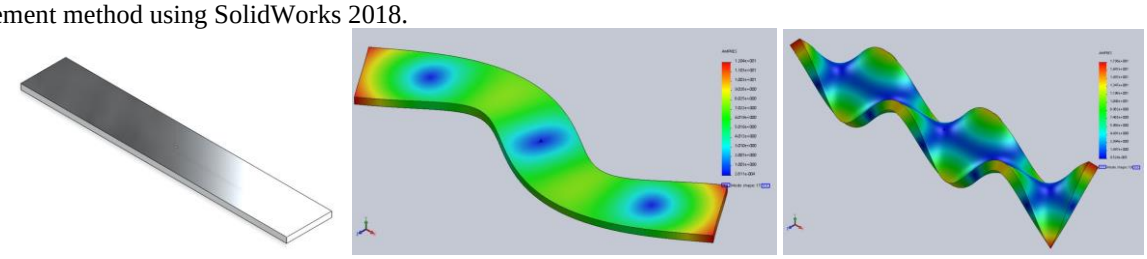

a b c

Figure 2: RUS spectrum for the main vibrational modes: b) extensional mode; c) flexural mode

The amplitude of signal in the swept frequency range are in tight connection with properties of the sample.

3. 2D ARCHITECTURE OF SENSORS

The experience gained in the construction and testing of linear eddy current sensor used for emphasizing the surface discontinuities in conductive materials [15, 16] leads to development of a 2D sensors able to detect and locate the flaws with a minimum of steps in scanning the inspected surfaces.

Consider a 2 D structure of sensors array [17] with one rectangular emission coil placed parallel with the surface to be inspected, driven by an alternative current that assures the electromagnetic field scattered into conductive material. The geometry has been simulated starting from the Green dyadic functions and the methods of integral volume [18]. The architecture has been designed as configurable, able to interrogate also only few reception coils by programming the data acquisition board. The 5x5 identical reception coils form an array, each line can work independently [19], and can be simultaneous interrogated by a multiplexer (figure 3).

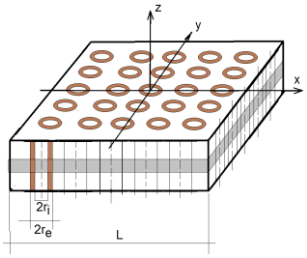

Figure 3: Scheme of the sensors array.

A multiplexing internal system reduces the mutual inductance and calculate the effective time for interrogation of the coils. The reception coils detect the field created by the emission coil and scattered by the discontinuities from the sample, the system measuring the recaptioned signals both in amplitude and phase.

4. MODELING AND SIMULATION OF ARRAY BEHAVIOR

Finite-difference time-domain offer a solution for the sensor's electromagnetic excitation at high frequencies. Using the system presented in Figure 3, using XFDTD software, the behavior of the architecture has been simulated. The FDTD algorithm is used as instrument for numerical evaluation in space and time of induced currents into Al2024 specimen. FDTD finds approximate solutions of Maxwell equations in differential forms, the discretization using the central difference through 30 approximations to the space and time partial derivatives. The equations are implemented in the software and solved in a cyclic manner: the electric field vector components in a volume of space are solved in time, the magnetic field vector components in the same spatial volume are successively solved. The process is repeated until the desired EM field state as transient or steady-state is fulfilled.

The field decrease exponential in time inside the material, being scattered by the discontinuity. Thus, a gradient along z axis will appear, allowing the identification of electric/magnetic field location of the peaks, corresponding to the position of discontinuity under the reception coils. Using FDTD, it is possible to test the design data implemented in simulation as well as the eventually improvement of geometrical elements and the performance of the axial gradient system taking into consideration the electromagnetic fields obtained in modelling. The discretization of the computational problem is given by Δx, Δy, Δz and corresponding, the permittivity, the permeability and the conductivity defined in the center of the Yee cell [20], where the electric and magnetic fields are defined at discrete points, each electric field component is located a half-cell width from the origin. The fields are manifesting in the center of each coil in the array. The scanning of the surface is made in "leap-frog" style, the step being equal with the width of the array. A current source represented by the emission coil creates the excitation field, being scattered into the sample, and the intensity was 0.1A at 130kHz frequency. The differences of the electric and magnetic field amplitudes received by the array in the presence of the sample with fatigue crack are presented in Figure 4.

The amplitudes of the fields are different for each location of the coils in the array and is in function of the location of discontinuity under certain coils, the amplitude being reduced at a distance larger than 3 times the minimum distance between the coils. The FDTD method allows the calculation of electromagnetic field generated into a small space, impossible to be carried out with analytical methods.

The perfect matched layers boundary conditions in FDTD simulation allow a high accuracy of the results.

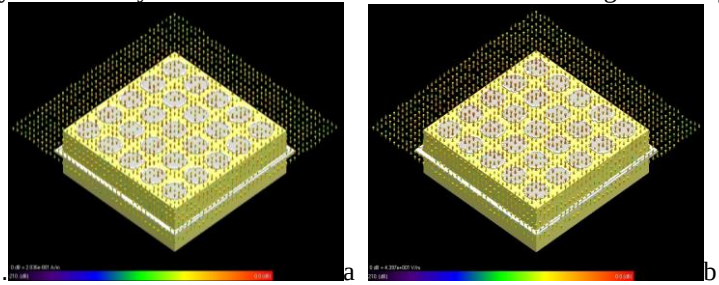

Figure 4: Simulation of electromagnetic fields in FDTD: a) Hz; b) Ez

Despite the fact that there are 5x5 coils, the interaction of each can be represented as a transfer of energy towards free space. The electromagnetic waves have a good distribution, each responding separately when each coil has a certain position toward the inspected surface. Also, the simulation allows the better choice of the architecture's sensors dimensions and layout to improve array's resolution.

5. SIGNAL PROCESSING SCHEME

For the start the reception coils was considered that form a linear array and is used for scanning over the fatigue crack. Using the direction of propagation method, the resolution of the sensors is improved [21]. The reception signals can be written as a vector

$$x_i = a_i e^{j\Psi_i} \quad i = 1,\cdots,M\ ; \begin{bmatrix} x_1 \\ \cdot \\ \cdot \\ x_M \end{bmatrix} = \begin{bmatrix} a_1 \\ \cdot \\ \cdot \\ a_M \end{bmatrix} \cdot \begin{bmatrix} e^{j\Psi_1} \\ \cdot \\ \cdot \\ e^{j\Psi_M} \end{bmatrix} \tag{2}$$

where M is the number of reception coils, $a1 \ldots aM$ and $\psi 1 \ldots \psi M$ are the amplitudes and phases of induced electromotive force for each element, and j is the unit imaginary number.
In order to locate discontinuities, the array manifold should be free of ambiguity [22]. Thus, the system won't be able to discern between two discontinuities placed at different distance that give the same response, emphasizing them as only one discontinuity. For one discontinuity, first rank ambiguity can appear [21]. The first rank ambiguity can be avoided by a weighting vector **w**, which linear combines the output signal from the sensor array into single output signal **y**[23]

$$\mathbf{y}=\mathbf{x}\mathbf{w}H \tag{3}$$

where superscript H denotes the Hermitic [i.e., conjugate-transpose] operation and the sensitivity distribution of a sensor array must be a cosine function. Thus, the maximum sensitivity occurs at the center of the array while on the boundary this is null. Each coil has been sampled in 12 intervals. The sensitivity at the center depends on the amplitude and phase of the current circulating in the emission coil when the array is placed over a good region. The power of a signal received by the array is proportional to the

$$\mathrm{P} \sim |\mathrm{y}|^2 \tag{4}$$

and the normalized response array [NRA] is defined as

$$\mathrm{NRA[dB]} = 10 \lg \frac{\mathrm{P} - \mathrm{P}_0}{\mathrm{P}_0} \tag{5}$$

where P_0 is the power at a reference point

$$\mathrm{P}_0 \sim |\mathrm{y}_0|^2 \tag{6}$$

and y_0 is the reference output array signal measured from a defect-free region. The normalized response array can be use to estimate the location of discontinuities.
Figure 5 presents the amplitude and the phase of the signal received by the linear eddy current sensors at the scanning over a notch, when the notch is found by the coil #3 and #4 from the array.

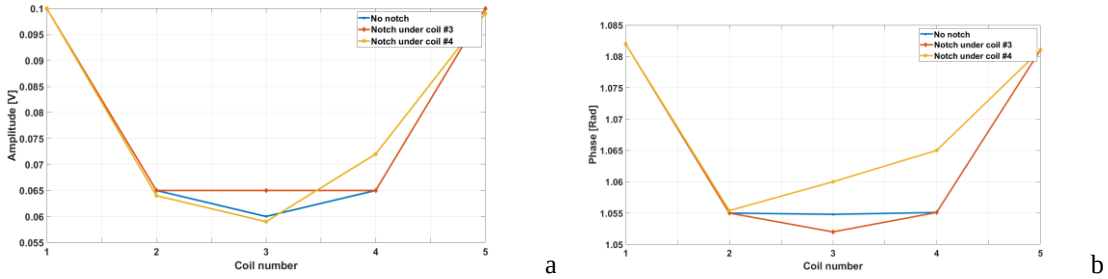

a b

Figure 5: The signal received by the linear array: a) Amplitude; b) Phase

It can be shown that the presence of a notch under a specific coil can be emphasized.
The signal processing scheme can be adapted to a sensor array by modelling the operation with dyadic Green's functions and obtaining the weight vector for different positions of the notch under specific reception coils from the array [17].

6. EXPERIMENTAL RESULTS

The incident magnetic field is assured by an emission coil, a rectangular frame with 6x6mm sides, having 100 turns. The emission coil is fed by a function generator WW1074 Tabor Ltd. The signal is amplified by Power amplifier RF A1012 AG-T&C Power Conversion Inc. The reception coils are connected to a multiplexor, which significantly increases the number of sensors that can be measured by a datalogger, improving also the scanning time.
The output signal is amplified, the reference signal being in the same phase with the input current into the emission coil. The amplifier delivers both the amplitude and the phase of the induced electromotive force [24]. The interrogation of reception coils is correlated with the scanning steps and speed, in order to have enough time for the temporary buffer to be emptied. The received signal is forwarded to the PC. The displacement system, the emission system and the reception part are controlled by codes developed in Matlab. The sample is displaced under the fixed sensor array with a XY scanning system, Newmark USA. The electromagnetic image of the scanned surface has been obtained by postprocessing of the signals acquired by each coil in each scanning point, using a sub encoding reconstruction algorithm and multiple coil scheme [25]. The image reconstruction starts at the first scanning step with the set of received signals using a low number of phase-encoding gradient steps. Applying Fourier transforms, aliased component images are obtained. Now, the signals are processed as images taking into account that each pixel in an aliased image is a superposition of multiple pixels [26, 27].
Figure 6 presents the response of sensors array at the scanning of studied sample, after signal post processing. It can be shown the presence of the crack under reception coils 3.3 and 3.4 (middle row).

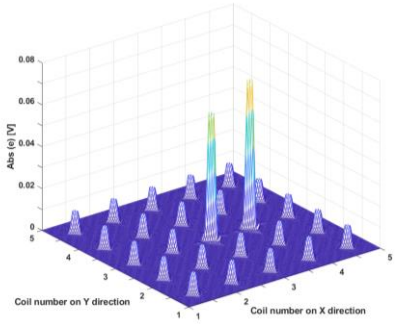

Figure 6: The response of the sensor array at the scanning over the fatigue crack in the sample

The length of a crack is evaluated upon the largest signals delivered by the reception coils at the crack's edge, meaning that the crack is directly evaluated from the spatial distance between the centers of two reception coils whose signals are clearly maximal. Initial results of applying the algorithm to the array data allows the localization of the fatigue cracks.

7. CONCLUSIONS

The mechanical properties of an aluminum plate as precursor for TBC support to be used in automotive parts were determined by ultrasound measurements. The vibration modes were simulated to determine the optimal frequencies for Resonant Ultrasound spectroscopy. The paper presents the methods to investigate the behavior of an aluminum plate in the presence of an inherent fatigue crack using a new type of electromagnetic sensors array. The model and the simulation of the 2D architecture are developed in order to extract the characteristic signal due to the presence of discontinuities under the surface of the studied specimen. The study of the dependence of the field distribution on the number and position of the reception coils against the discontinuity was carried out using FDTD. The 2D architecture has been designed and experimental test have been carried out in order to verify the possibility to obtain the distinct answer of each reception coil to a certain position of the discontinuity. The presented results show that the electromagnetic signal obtained by simulation coincides with the experimental one, suggesting that the 2D structure can assure the scan in leapfrog step of the surface with small dimensions, précising the location of the discontinuity. Further tests will be complete after deposition of TBC with bond coat in order to emphasize the influence of TBC on the signal received by the array.

ACKNOWLEDGMENTS

This work was partially supported by Romanian Ministry of Education and Research, Nucleus PN 19 28 01 02 and Bilateral Cooperation JINR under protocol 24-4-1121-2015/2020.

REFERENCES

[1] Kumar D., Pandey K.N. and Das D.K., 2014. Thermal barrier coatings on aluminium-based alloy 2024 for high temperature protection subjected to thermal cyclic loading. Procedia Materials Science, 5, pp.1075-1080.
[2] Schlesier C., Nembach E., 1995 Strengthening of aluminium-lithium alloys by long-range ordered δ'-precipitates. Acta metallurgica et materialia 43(11)3983-3990
[3] Belov N.A., Eskin D.G., Aksenov A.A., 2005 Multicomponent phase diagrams: applications for commercial aluminum alloys (Elsevier Ltd).
[4] Miller, W.S., Zhuang, L., Bottema, J., Wittebrood, A., De Smet, P., Haszler, A. and Vieregge, A.J.M.S., 2000. Recent development in aluminium alloys for the automotive industry. Materials Science and Engineering: A, 280(1), 37-49.
[5] Parker DW. 1992, Thermal barrier coatings for gas turbines, automotive engines and diesel equipment. Materials Design; 13, 345–351
[6]https://www.makeitfrom.com/material-properties/2024-AlCu4Mg1-3.1355-2L97-A92024-Aluminum last seen on March 1st, 2020.
[7] Brahami A., Bouchouicha B., Zemri M. and Fajoui J., 2020. Fatigue crack growth rate, microstructure and mechanical properties of diverse range of aluminum alloy: a comparison. Mechanics and Mechanical Engineering, 22(4), 1453-1462.
[8] Felice M.V., Velichko A., Wilcox P.D., 2014 Accurate depth measurement of small surface-breaking cracks using an ultrasonic array post-processing technique NDT & E International 68 , 105-112
[9] Chlada M., Prevorovsky Z., 2012 Remote AE monitoring of fatigue crack growth in complex aircraft structures. Algorithms 3(4): 5
[10] Lemaitre J., Dufailly J., 1987 Damage measurements Engineering Fracture Mechanics 28 643-661
[11] Krautkrämer J., Krautkrämer H., 1990 Ultrasonic testing by determination of material properties. In Ultrasonic Testing of Materials pp 528-550 (Berlin: Springer).
[12] ASTM B646 – Fracture toughness testing of aluminum alloys
[13] Noroozi A.H., Glinka G., Lambert S.,2005 A two-parameter driving force for fatigue crack growth analysis International Journal of Fatigue 27 pp 1277–1296
[14] Leisure, R.G. and Willis, F.A., 1997. Resonant ultrasound spectroscopy. Journal of Physics: Condensed Matter, 9(28), p.6001.
[15] Mook G., Michel F., Simonin J. 2011 Electromagnetic imaging using probe arrays Strojniški vestnik-Journal of Mechanical Engineering 57(3) pp 227-236
[16] Mihalache O., Grimberg R., Radu E., Savin A., 1997 Finite element numerical simulation for eddy current transducer with orthogonal coils Sensors and Actuators A: Physical 59(1-3) pp 213-218
[17] Grimberg R., Udpa L., Savin A., Steigmann R., Palihovici, V. and Udpa, S.S., 2006. 2D Eddy current sensor array. Ndt & E International, 39(4), pp.264-271.
[18] Radu E., Grimberg R., Savin A., Mihalache O., 1997 Modelling the operation of the eddy current transducer with orthogonal coils in the presence of material discontinuities, Sensors and Actuators A: Physical 59(1-3) 201-204
[19] Grimberg R., Wooh S.C., Savin A., Steigmann R., Premel D., 2002 A linear eddy current array transducer for rapid high-performance inspection INSIGHT 44(5), 289-293.
[20] Yee K 1966 Numerical solution of initial boundary value problems involving Maxwell's equations in isotropic media IEEE Transactions on antennas and propagation 14(3) 302-307
[21] Cadzow, J.A, 1993. The signal subspace direction-of-arrival algorithm. Handbook of Statistics, 10,127-157.
[22] Shiavi, R., 2010. Introduction to applied statistical signal analysis: Guide to biomedical and electrical engineering applications. Elsevier.
[23] Shell SV, Gardner WA 1993 High Resolution Direction Finding Handbook of Statistics, Vol.10, Ed. NK Bose and CR Rao, Elsevier.
[24] Mook G., Lange R., Koeser O., 2001 Non-destructive characterisation of carbon-fibre-reinforced plastics by means of eddy-currents Composites science and technology 61(6) 865-873
[25] Wang J., Liang J., Cheng J., Guo Y., Zeng L., 2020 Deep learning-based image reconstruction algorithm for limited-angle translational computed tomography, Plos one 15(1), p.e0226963.
[26] Sodickson DK 2007 Spatial encoding using multiple RF coils: SMASH imaging and parallel MRI Encyclopedia of Magnetic Resonance (John Wiley & Sons, Ltd.)
[27] Balanis CA 2005 Antenna theory: analysis and design. 3rd ed. (New Jersey: John Wiley & Sons)